Mechanisms of Fatigue Damage Formation and Evolution in Zr-Based Bulk Metallic Glass

Peter A. Hess, Brian Menzel and Reinhold H. Dauskardt

Department of Materials Science and Engineering
Stanford University
Stanford, CA 94305-2205

ABSTRACT

Zr-based bulk metallic glasses (BMGs) are surprisingly susceptible to cyclic fatigue processes. However, the mechanisms of fatigue damage initiation and evolution in bulk metallic glasses (BMGs) are not well understood, limiting their use in safety-critical structural applications. We present recent experimental and modeling studies of both the initiation of fatigue damage obtained from stress-life experiments on smooth specimens, and the growth of fatigue cracks measured under stable and transient cyclic loading conditions.

INTRODUCTION

Zr-based bulk metallic glasses (BMGs) exhibit remarkable mechanical properties under monotonic loading [1-7], but appear to be surprisingly susceptible to fatigue processes under alternating loads [4, 8]. A low fatigue crack-growth threshold, ΔK_{TH}, and endurance limit, σ_e, under cyclic loading are among the foremost concerns for structural applications. The mechanisms of fatigue crack initiation and propagation in metallic glasses are currently not well-understood in terms of the underlying shear banding processes.

Accordingly, the evolution of fatigue damage was experimentally characterized in terms of both "small" and "long" fatigue crack growth rate behavior to elucidate the detailed mechanism of fatigue crack growth. The sub-T_g elevated temperature fatigue crack propagation behavior was examined [9]. The fatigue threshold, ΔK_{TH}, was found to increase from ~1.1 MPa-m$^{1/2}$ to ~1.4 MPa-m$^{1/2}$ as testing temperature was increased from 100°C to 220°C. Low levels of fatigue crack closure were apparent and not associated with threshold behavior.

High resolution characterization of fatigue fracture surfaces were used to provide the basis for micromechanical models of the resulting fatigue mechanisms. Regular arrays of micron-sized elongated ridges formed parallel to the crack growth direction in the near-threshold fatigue crack-growth regime at elevated temperatures. Unlike the meniscus instability mechanism that has been used to explain fracture processes, a new mechanism involving crack front stability and out-of-plane shearing processes is used to rationalize the observed fatigue behavior. A model for ridge formation based upon the planar stability of a Mode I crack was proposed. Ridge wavelengths and amplitudes were accurately predicted with respect to changes in applied stress intensity and temperature, and ridge angles were calculated on the basis of a Mohr-Coulomb yield criterion.

The effects of alternating loads on the flow and damage processes of a Zr-based BMG was also investigated using stress-life fatigue tests conducted using a bend specimen under tension-tension loading [10]. The formation and growth of defects was monitored on the maximum tensile surface of the bend specimens using a surface replicating technique. Damage initiation sites mostly associated with pre-existing defects such as second phase inclusions or surface roughness were found by tracing back through the surface replicas made during fatigue testing. Damage was observed to initiate as shear bands or mixed mode cracks after only a few stress cycles which propagated at ~ 49^o to the maximum normal stress axis. Surprisingly, they all abruptly changed orientation after reaching a critical length, and grew as mode I cracks until failure. The growth rate of these "small" surface cracks was measured and used in predictions of the expected fatigue life. It is demonstrated that damage initiation appeared to have little contribution to the fatigue life. The intent of the present study was therefore to identify and elucidate the fatigue damage mechanisms in BMG's particularly in the early stages of fatigue life, and to provide an explanation for the anomalously low fatigue endurance limits reported.

EXPERIMENTAL

Compact tension fatigue specimens with width W = 38.1 mm and thickness B = 3.1 mm were wire electro-discharge machined from as-cast plates of $Zr_{41.25}Ti_{13.75}Cu_{12.5}Ni_{10}Be_{22.5}$ BMG (Vitreloy 1, Liquidmetal Technologies, Lake Forest, CA) with dimensions in general accordance with the ASTM-E647 standard for measurement of fatigue crack growth rates. Testing was performed inside a temperature-controlled environmental chamber (± 0.5°C). Fatigue crack-growth rates, *da/dN*, were measured under decreasing applied stress-intensity range ($\Delta K = K_{max} - K_{min}$) conditions, using an automated load-shedding technique on an electro-servo-hydraulic mechanical testing system, in general accordance with ASTM-E647.

Stress-life tests were conducted on rectangular specimens 3 mm x 3 mm in cross-section and 40 mm long. The specimens were mechanically polished on all faces to a final RMS surface roughness of 0.1 µm. The corners of the beam were slightly rounded to reduce stress concentration along the edge of the specimen. Specimens were loaded using a fully articulating four-point bend fixture with an outer, So, and inner, Si, span of 30 and 10 mm, respectively, in a servohydraulic mechanical test system. Testing was conducted at a nominal frequency of 5 Hz except for a high cycle fatigue test that was conducted at 50Hz under load control using a sinusoidal waveform and a load ratio of R = 0.1.

Fracture surfaces were examined using scanning electron microscopy (SEM), atomic force microscopy (AFM), X-ray photoelectron spectroscopy (XPS), and transmission electron microscopy (TEM) to characterize the fractography and surface composition of polished, fatigue, and fracture surfaces. X-ray diffraction was performed on the specimen tested at 220°C and compared to the as-cast plate to ensure that crystallization of the material did not occur at the elevated testing temperature.

RESULTS and DISCUSSION

Elevated temperature fatigue crack-growth rates, measured at temperatures of 100°C, 140°C, 180°C, and 220°C are plotted as a function of applied ΔK in Figure 1 [9]. A distinct mid-growth rate regime was apparent together with decreased growth rates in the near-threshold region. However, a distinct threshold region characteristic of most crystalline metallic materials was not apparent. The mid-range growth rates could be fitted to a Paris power law relationship. Fatigue threshold values, ΔK_{TH}, were found to increase with testing temperature.

Fatigue striations were visible over regions of the crack surface for the entire range of growth rates for the specimens tested at 220°C and at growth rates above ~10^{-9} m/cycle for all other specimens, although they do not uniformly cover the surface. Models for striation formation assume that a single loading cycle produces a single striation. However, the spacing of observed striations was ~10-100 times greater than the measured growth rates.

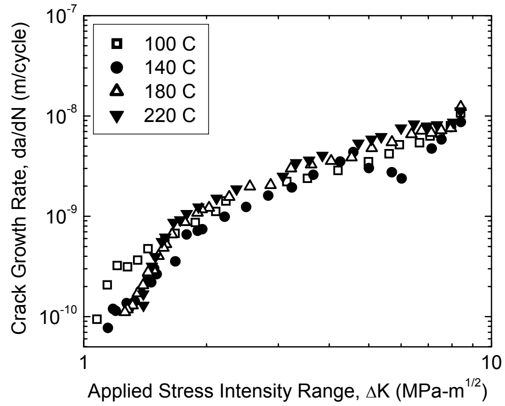

Fig. 1: Mode I fatigue crack-growth data for Vitreloy 1 tested at various temperatures.

A surprising observation in the present study was the development of elongated ridges running parallel to the direction of crack propagation as the testing temperature was increased, as shown in Figure 2. The ridges increased in size and spacing with increasing temperature and applied ΔK, before they begin to break up at higher growth rates. The wavelengths of the ridges were measured and modeled in terms of the out-of-plane stability of the crack front. Previously published studies of the stability of a crack front suggest that without microstructural barriers, wavy crack front formation is favorable in the presence of positive T-stress [11]. In the present metallic glass, we show that such ridges are produced, and that their shape satisfies a Mohr-Coulomb yield criterion. In addition, we also show that the resultant wavelength is proportional to the crack tip opening displacement.

The number of cycles to failure, N_f, measured as a function of the normalized applied stress amplitude, σ_a/σ_{UTS}. The results are consistent with published results for a similar metallic glass [5,10]. The endurance limit was found to be $\sigma_a/\sigma_{UTS} = 0.05$. It was still less than 10% of the ultimate tensile strength and in stark contrast to typical high strength polycrystalline metals which exhibit endurance limits of ~ 0.5 σ_{UTS}.

Examination of the replicas revealed a distribution of surface cracks that evolved in size and density with increasing number of loading cycles as shown in Fig. 3(a). The damage originated in multiple locations on the tensile surface or at the corner between the tensile surface and the side of the beam. All surface damage appeared to originate from pre-existing flaws in the specimen. Although the type of defect (e.g. scratch, sub surface void, surface pit or second phase inclusion) could not be determined unambiguously, it appeared that surface scratches play a key role in the initiation of defects. Damage was observed to initiate as shear bands or mixed mode cracks after only a few stress cycles which propagated at ~ 49^o to the maximum normal stress axis (Fig. 3(b)). Surprisingly, they all abruptly changed orientation after reaching a critical length, and grew as mode I cracks until failure. The critical length at which the damage abruptly changed orientation was in the range 40 – 70 μm depending on load level. The orientation angle of the initial damage with respect to the tensile axis was found to be ~ 49°.

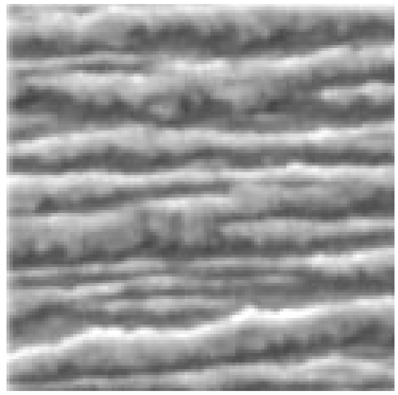

Fig. 2: Micrograph of fatigue crack surface ridges from a specimen tested at 220°C K. Crack growth direction is from left to right.

Using numerical solutions reported for semi-elliptical cracks under mixed mode loading conditions the stress intensities along the crack front were calculated as a function of crack length for both surface and edge cracks. The transition from the angled shear band to the mode I crack was modeled in terms of the critical Mode I stress intensity factor needed to exceed the Mode I ΔK_{TH}. The growth of the initial shear bands and subsequent cracks was carefully measured and the resulting small crack growth rates determined as a function of the applied stress intensity factor. The small crack growth rates were found to be consistent with the long crack growth behavior, indicating that no anomalous small crack growth rate behavior was apparent. Fatigue life was estimated from the observed initial defect sizes, and predictions were found to be consistent with measured stress life data.

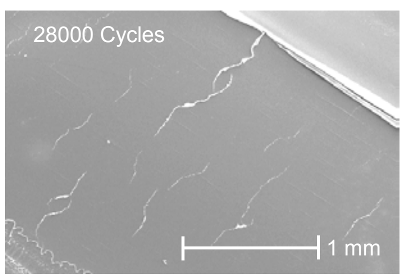

(a)

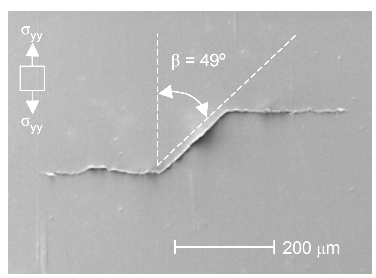

(b)

Fig. 3: SEM of surface replicas showing (a) distributed damage on the specimens tensile surface, and (b) magnified image of the surface damage.

CONCLUSIONS

The effect of elevated temperatures below the glass transition temperature (T_g) was examined on the fatigue crack propagation behavior of a Zr-based BMG. Near-threshold fatigue crack propagation rates were found to decrease, and fatigue thresholds increased, with increasing testing temperature. Low levels of fatigue crack closure were apparent at all test temperatures and were not important in affecting the resulting thresholds. The fracture surface morphology revealed the presence of a regular pattern of elongated ridges parallel to the crack growth direction during near-threshold growth at elevated temperatures. Flow-based meniscus instability models were not able to describe the ridge formation. A model based upon the planar stability of a Mode I crack in the through-thickness direction was proposed based on existing mechanics solutions for crack front stability.

During stress-life testing, damage was observed to initiate as shear bands or mixed mode cracks after only a few stress cycles from pre-existing defects such as second phase inclusions or surface roughness. The apparent lack of a damage initiation stage may account for the low endurance limit reported for this material, ~1/10 of the ultimate tensile strength. The resulting "small" fatigue crack growth rates were carefully characterized and shown to be consistent with "long" crack growth rate behavior indicating the absence of significant crack tip shielding.

ACKNOWLEDGEMENTS

This work was supported by the MRSEC program of the National Science Foundation under award No. DMR-0080065, and by a CALTECH subcontract (1036235-01) of the DARPA-DSO-SAM program.

REFERENCES

1. H.A. Bruck, T. Christman, A.J. Rosakis, and W.L. Johnson. Scripta Metallurgica et Materialia, 1994. **30**(4): p. 429-34.
2. R.D. Conner, A.J. Rosakis, W.L. Johnson, and D.M. Owen. Scripta Materialia, 1997. **37**(9): p. 1373-8.
3. K.M. Flores and R.H. Dauskardt. Scripta Materialia, 1999. **41**(9): p. 937-43.
4. K.M. Flores and R.H. Dauskardt. in *Supercooled Liquid, Bulk Glassy and Nanocrystalline States of Alloys*. 2000. Boston, MA, USA: Mater. Res. Soc. 2001
5. C.J. Gilbert, R.O. Ritchie, and W.L. Johnson. Applied Physics Letters, 1997. **71**(4): p. 476-8.
6. P. Lowhaphandu and J.J. Lewandowski. Scripta Materialia, 1998. **38**(12): p. 1811-1817.
7. X. Rao, P.C. Si, J.N. Wang, Z. Xu, S. Xu, W.M. Wang, and W.H. Wang. Materials Letters, 2001. **50**: p. 279-283.
8. C.J. Gilbert, J.M. Lippmann, and R.O. Ritchie. Scripta Materialia, 1998. **38**(4): p. 537-42.
9. P. A. Hess and R. H. Dauskardt, Acta Materialia, 52 (12): 3525-3533, 2004.
10. B. Menzel and R. H. Dauskardt, "Fatigue Damage and Endurance Limits of a Zr-Based Bulk Metallic Glass," Acta Materialia, 2004. To be submitted.
11. H. Gao. Journal of Applied Mechanics, 1992. **59**: p. 335-343.